ACS Sustainable Chemistry & Engineering

Research Article

pubs.acs.org/journal/ascecg

Formation and Characterization of Fully Dilutable Microemulsion with Fatty Acid Methyl Esters as Oil Phase

Wanxu Wang,*[,†] Hongtu Wei,[†] Zhiping Du,*[,†,‡] Xiumei Tai,[†] and Guoyong Wang[†]

[†]China Research Institute of Daily Chemical Industry, No. 34 Wenyuan Road, Taiyuan 030001, People's Republic of China

[‡]Institute of Resources and Environment Engineering Research Institute, Shanxi University, No. 92 Wucheng Road, Taiyuan 030006, People's Republic of China

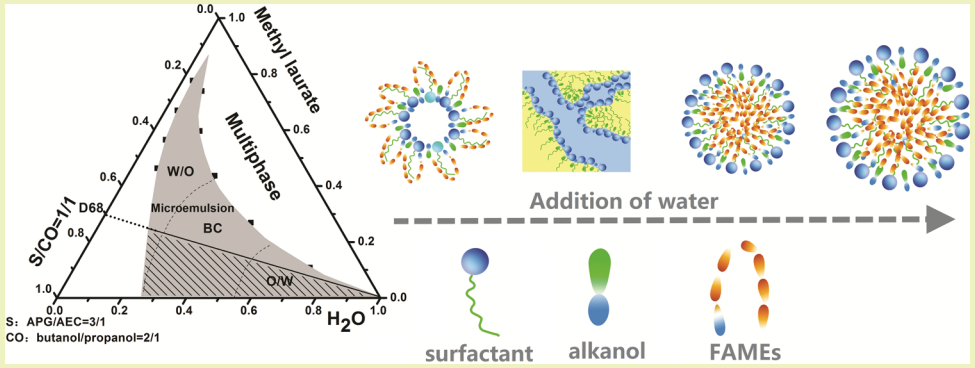

ABSTRACT: The objective of this study was to develop a green microemulsion with potential applications in the delivery system for oil-soluble solid active ingredients. A microemulsion was prepared using fatty acid methyl esters (FAMEs) as the oil phase, a mixture of alkyl polyglycoside (APG) and alkylpolyethoxy carboxylates (AEC) as the surfactant, and alkanol as a cosurfactant. The feasibility of formulating a fully water dilutable microemulsion with a green surfactant and nontoxic oil phase has been demonstrated. Pseudoternary phase diagrams were constructed by titration, and a large isotropic region was found. To expand the isotropic regions area, the effect of the mixing ratio of APG and AEC, the chain length of the cosurfactant and the oil on the isotropic area of the phase diagram were investigated systematically. As the water content increased, the continuous structural transition from water-in-oil, bicontinuous to oil-in-water microemulsion was followed by monitoring conductivity. Percolation phenomena were observed during this process. Based on the phase behavior study, the optimum formulations were chosen from isotropic regions with a minimum amount of surfactants, which were able to be fully diluted with water. The dilute microemulsion was studied by dynamic light scattering (DLS), dynamic contact angle and dynamic surface tension. The DLS result revealed that the main destabilization mechanism for these dilute microemulsion was Ostwald ripening at the beginning of the dilution process. Dynamic contact angle and dynamic surface tension results demonstrated the dilute microemulsion exhibited excellent wetting and spreading properties on hydrophobic surfaces.

KEYWORDS: *Fully water dilutable microemulsion, fatty acid methyl ester, delivery system*

INTRODUCTION

Microemulsions, which are thermodynamically stable isotropic liquids, can be formed spontaneously by mixing oil, water and surfactant (and/or cosurfactant) together.[1−4] Besides, a microemulsion can be formed spontaneously depending on composition and environmental conditions (particularly temperature). Colloidal dispersions systems, such as microemulsions, have attracted considerable attention in transport of water-insoluble active ingredients in the agrochemical,[5−7] pharmaceutical[8−10] and food industries[11−13] for a long time. Systems containing nanoscale aggregates (radius < 100 nm) can also encapsulate and deliver biologically active ingredients,[11,14,15] such as pesticide, drugs, vitamins and antimicrobials.

Up to now, there are several notable challenges related to the application of microemulsions.[13] One is that large quantities of surfactants are required for the preparation of a microemulsion. High surfactant concentration will render them relatively expensive. Another one is that the oil phase in the microemulsion may also be toxic, flammable, or contain volatile organic solvents, necessitating safety measures. It has also been proven very difficult to prepare microemulsions that can be fully diluted in water, or cannot be stable when diluted with water. Instead of a single surfactant, mixtures of surfactants have been used to reduce the total amount of surfactant in each microemulsion, to extend the single phase region and to enhance the stability on shifts in temperature and salinity.[16] Especially, mixtures of nonionic and ionic surfactants can

Received: September 18, 2014
Revised: December 30, 2014
Published: January 29, 2015

DOI: 10.1021/sc500667n
ACS Sustainable Chem. Eng. 2015, 3, 443−450

produce synergistic effects, allowing the formation of temperature-insensitive microemulsions.[17] It has also been shown that it is possible to increase the oil solubilization capacity through the use of a suitable surfactant and by the addition of polyols and short-chain alcohols.[12] The dilutability of microemulsions is a primary concern for their use as delivery system.[18] The dilution procedure and the microemulsion composition, chain length of cosurfactant and oil all have important effects on the size and polydispersity[18,19] of the dilute microemulsion.

Due to the requirements of green chemistry and engineering, it is necessary to formulate and characterize microemulsions based on the biocompatibility of surfactants and renewable and nontoxic oils. Environmentally friendly alkylpolyglucosides (APG) have desirable characteristics including excellent biodegradability, no environmental toxicity, better biocompatibility and temperature insensitivity.[20] In recent decades, microemulsions using APG as a surfactant have been studied extensively. Kahlweit and co-workers investigated phase behavior of alkylpolyglucoside stabilized microemulsion and discussed the function of *n*-alkanols in these system.[21] T. Sottmann has described the phase behavior of water/*n*-octane/C8G1/*n*-octanol.[22] To obtain a nontoxic microemulsion, M. Kahlweit used unsaturated fatty acid ethyl ester as the oil, a long-chain soy bean lecithin as the amphiphile, and pentane-1, 2-diol as the cosolvent.[21] Nowadays, an intermediate polarity groups such as poly(ethylene oxide) (EO) chain has been inserted between the hydrophilic head and the hydrophobic tail of the surfactant, such as alkylpolyethoxy carboxylates (AEC). With the presence of these intermediate polarity groups, the surfactants possess the ability of both anionic and nonionic surfactant, which results in stronger interaction with both oil and water phases.[23] Due to the unique molecular structure, these surfactants can form a thickening of the interfacial region and offer a smooth polarity transition zone between two bulk phases. This kinds of surfactant molecular may favor the formation of a stable and efficient microemulsion. Fatty acid methyl esters (FAMEs), known as "green solvents", are obtained by transesterification of renewable biological resources such as vegetable oils with methanol.[2] FAMEs based microemulsions have already been produced and used as microemulsion fuels and pesticide microemulsion formulation.[24] The advantages in the formulation of microemulsions with FAMEs are their nontoxic, rapid biodegradability in soil, low vapor pressure and noninflammability, high flash point, etc.

Here, we present a fully water diluted green microemulsion using the mixture of green surfactant APG and AEC as surfactants, medium-chain alkanols as cosurfactants and FAMEs to provide the oil phase. The regions of single phase microemulsion in the model system water/APG-AEC/alkanol/FAMEs were found by drawing pseudoternary phase diagrams. The changes in the microstructure of the system were analyzed using conductivity. The dilution stability of microemulsions was explored by dynamic light scattering. The spreadability and wettability of the dilute microemulsion was characterized by dynamic contact angle and dynamic surface tension. We propose that our microemulsion might find use as a carrier in pesticide formulations.

EXPERIMENTAL SECTION

Materials. All fatty acid esters (palmitic acid methyl ester, methyl laurate, oleic acid methyl ester) were purchased from Nanjing Hand of Hand Chemical & Technology Co., Ltd. (Nanjing, P. R. China). Propanol (≥99.0%), glycerol (≥99.0%), butanol (≥99.0%) and amyl alcohol (≥99.0%) were purchased from Sinopharm Chemical Reagent Beijing Company Ltd. (Beijing, P. R. China). Dodecyl/tetradecylpolyglucosides (APG, >50%) with a degree of polymerization = 1.4, and fatty alcohol polyoxyethylene ether carboxylate (AEC, >98%) with an ethoxylation degree around 9 were both obtained from China Research Institute of Daily Chemical Industry. APG (>50%) was purified from a dispersion in absolute ethyl alcohol by distillation under vacuum followed by dying in vacuum oven at 40 ± 2 °C for 24 h to obtain a 99% powder. All other chemicals were used without further purification. Deionized water (18.2 MΩ) was used for all experiments.

Methods and Techniques. *Phase Diagram Determination.* The microemulsion region was determined with pseudoternary phase diagrams, which were constructed through the stepwise addition of water to concentrated stock solutions of oil, surfactant, and cosurfactant in different weight ratios. The mass ratio of total surfactant to cosurfactant (alkanol) (K_m) was kept constant at 1:1, whereas the mixture of them was set as an independent variable. A total of three grams of surfactant mixture, alkanol and FAMEs were weighted into a 10 mL screwable tube. *R*, the mass ratio of FAMEs to surfactant and cosurfactant, was set to 1:9, 2:8, 3:7, ..., 9:1, during each experiment. Water, the titration component, was progressively added drop by drop to the prepared mixtures at 25 ± 1 °C under a magnetic stirrer. Changes in the visual appearance of the sample, transparent-to-turbidity or turbidity-to-transparent transitions, was recorded as phase boundary. The procedure was repeated three times in each case, and the mean reported. Samples were allowed to equilibrate for at least 24 h prior to examination. Polarized filter were used to discern liquid crystalline phase. The composition of the sample was calculated from the weight measurement of all components, and then a pusedoternary phase diagram was constructed with these points.

In the second experiments, Water dilution experiments were carried out based on the optimum formulation, which was obtained from the pusedoternary phase diagram. The mixture of surfactant, alkanol and FAMEs was mixed by a given value of *R*. Then, the mixture was progressively diluted with an aqueous phase (added drop by drop). If the system remained transparent upon further dilution, the microemulsion was considered fully dilutable along dilution line investigated.

Microemulsion Characterization. *Conductivity Measurements.* The structure transition of microemulsion with increasing quantities of water was monitored through measurement the electrical conductivity. Electrical conductivity measurements were performed at 25 ± 0.1 °C using a low-frequency conductivity analyzer (model DDS-6700, Shanghai Rex Xinjing Instrument Co., Ltd.). Water was dropwise added to the microemulsion with magnetic stirring. The electrode was dipped in the microemulsion sample until equilibrium was reached and reading becomes stable. The conductivity was recorded as a function of water consumption. The reported conductivity values represent the mean of 3 measurements, carried out at intervals of 3 min after 10 min of stirring.

Droplet Size Measurements. Droplet size measurements were used to determine the dilution stability of dilute solution of microemulsions. The averaged droplet size was carried out using dynamic light scattering (Brookhaven, model BI-200SM, United States) at different dilution. To study microemulsion dilution stability, the dilution procedures were used by addition of microemulsion into water in one step with magnetic stirring. All of measurements were performed with various time of storage at 25 ± 0.5 °C with a scattering angle of 90°. All solutions were equilibrated at 25 ± 0.5 °C for 8 h prior to the experiments, and each measurement was repeated for three times.

Contact Angle Measurements. Contact angle measurements were used to measure the spreading of dilute solution of microemulsions onto hydrophobic substrates using drop shape analyzer DAS-100 (Krüss Company, Germeny). Paraffin film was chosen as solid substrates, as it shows different solid−air interfacial energies in terms of contact angles for water: (106 ± 2)° on Paraffin. The environmental humidity was maintained at 50 ± 5%. Each experiment was repeated at least three times. The mean contact angles is reported.

Dynamic Surface Tension Measurement. The dynamic surface tension was measured using a Krüss BP100 bubble-pressure tensiometer (Krüss Company, Germany). Prior to the measurements,

DOI: 10.1021/sc500667n
ACS Sustainable Chem. Eng. 2015, 3, 443−450

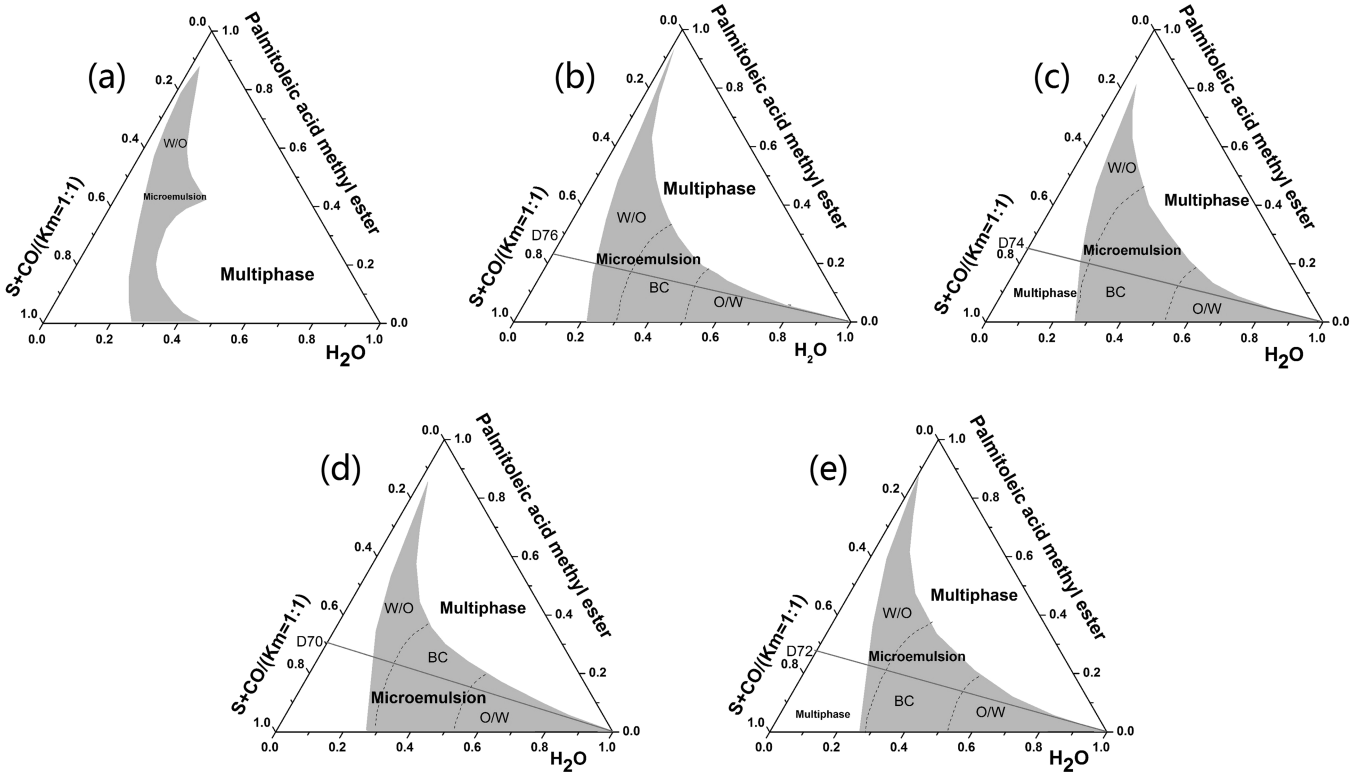

Figure 1. Pseudoternary phase diagrams for water/APG-AEC/1-butanol/palmitoleic acid methyl ester systems, APG/AEC in (a) 1:0, (b) 1:1, (c) 2:1, (d) 3:1 and (e) 4:1 at 25 °C and with K_m = 1:1. Gray areas represent the single phase microemulsion region. All compositions are shown as weight ratios.

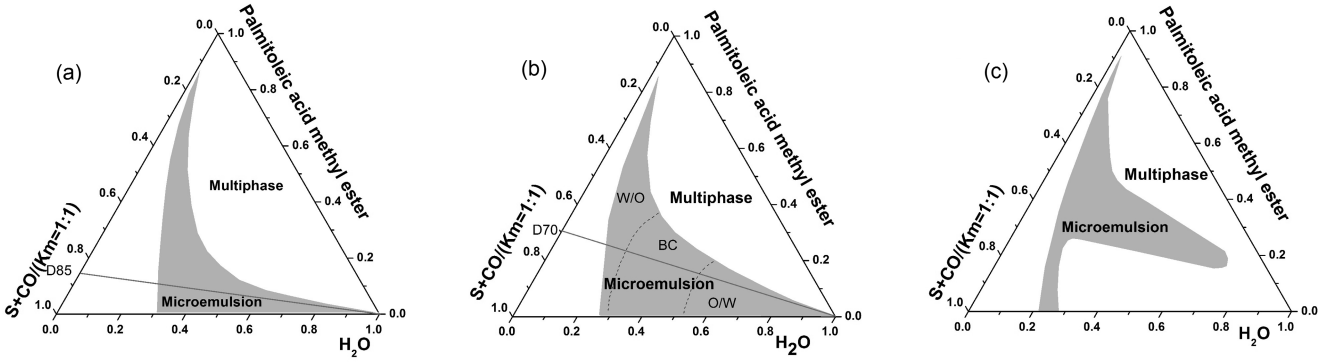

Figure 2. Pusedoternary phase diagram for water/APG-AEC/palmitoleic acid methyl ester and (a) 1-propanol, (b) 1-butanol or (c)1-pentanol at 25 °C and with K_m = 1:1 and APG/AEC=3/1. The gray areas represent the single phase microemulsion regions. All compositions are given as weight ratios.

calibration of the Instrument using double-distilled water was performed to ensure that no contamination was present in this system. This measurement was conducted with effective surface ages ranging from 10 to 50000 ms. Measurements were performed at 25 ± 1 °C.

RESULTS AND DISCUSSION

Phase Behavior. *Effect of APG-AEC Ratio.* Figure 1 shows the pseudoternary phase diagram for the water/APG-AEC/1-butanol/palmitoleic acid methyl ester system. The effect of the AEC to APG weight ratio on the area of single phase of microemulsion was discussed. In all the phase diagrams, the weight ratio of surfactant (AEC+APG) to cosurfactant (K_m) is constant (K_m = 1). The microemulsion region and multiphase region can be clearly divided, marked in Figure 1. The shaped part represents single microemulsion phase regions. It can be seen that using APG alone as surfactant only a narrow region of microemulsion phase could form (Figure 1a). There are no "diluting channels" that reach the water corner of the phase diagram cross the single phase region. With the addition of AEC together with APG, the mixtures of APG and AEC were used at the different mass ratio, from 1:1 to 4:1 (Figure 1b–e). It can be seen that single phase regions became obviously larger in Figure 1b–e. It seems that the single-tailed ionic surfactant, i.e., AEC, increases the efficiency of nonionic surfactant (APG) significantly.[17] Clearly, APG and AEC have a synergistic effect on expansion of the microemulsion phase region. All these phase diagrams have paths stretching to the water-rich corner cross the entire phase diagram. The optimum microemulsion regions were observed at 3:1 which have relatively wide channel

DOI: 10.1021/sc500667n
ACS Sustainable Chem. Eng. 2015, 3, 443–450

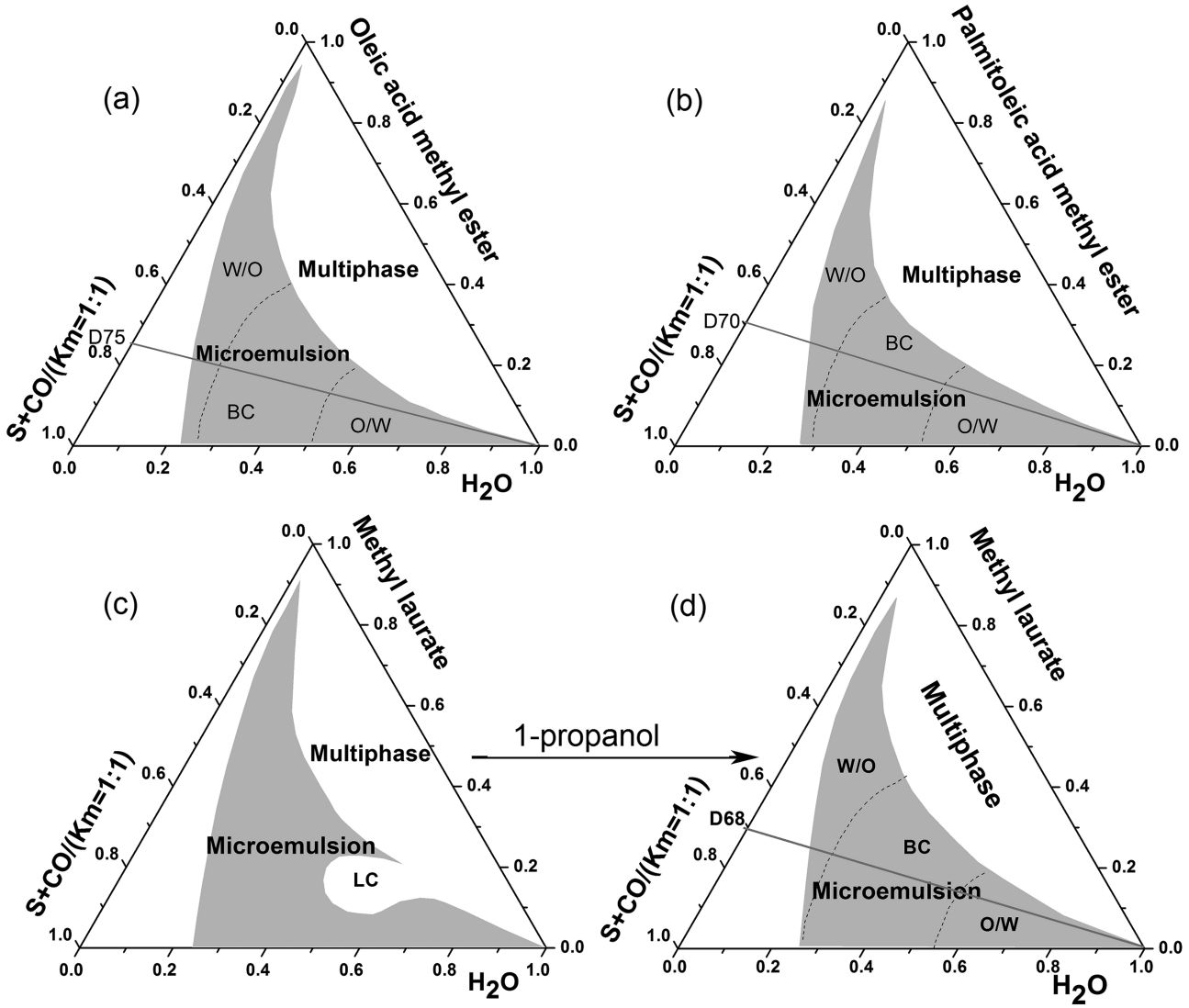

Figure 3. Pusedoternary phase diagrams for water/APG-AEC/1-butanol/(a)oleic acid methyl ester, (b) palmitic acid methyl ester or (c) methyl laurate at 25 °C and with APG/AEC=3/1; (d) water/APG-AEC/1-butanol&1-propanol/methyl laurate, 1-butanol/1-propanol=2/1. The gray areas represent the single phase microemulsion region. All compositions are shown as weight ratios.

toward the water rich zone. The results show that in the presence of AEC, the conformation of selective nonionic amphiphiles packing at interface layer of microemulsion droplets significantly change. Adding anions to nonionic systems induces an attractive interaction promoting the formation of mixed micelles and increasing the adsorption capacity for surfactants at the interface. Surfactant molecules are arranged more closely together at the interface, increasing the strength of the interface film and the stability of the droplets. Furthermore, anion and nonionic mixture system have two important features, namely, the system has less sensitive to temperature and salinity. This could afford the microemulsion more practical value as a pharmaceutical carrier. So, the optimum surfactant was the mixture of APG and AEC (3:1).

Effects of Cosurfactants. To investigate the effect of the chain length of linear alkanols as cosurfactants on the phase behavior of the water/APG-AEC/alkanol/FAMEs system, different alkanols were used in this section. Klossek et al. proposed that ethanol was added as cosolvent to enhance the film flexibility and so to increase the microemulsion area and the solubilization of FAMEs.[25,26] Figure 2a−c depicts the pseudoternary phase diagrams in which 1-propanol, 1-butanol and 1-pentanol were used as cosurfactants (K_m = 1:1), respectively. It can be readily observed that the areas of single phase regions are dramatically influenced by the chain length of cosurfactant. Replacing 1-butanol with 1-propanol, the single microemulsion region shrank (Figure 2a) and it shows that only the mass ratio of emulsifier to oil is larger than 85%, the microemulsion can be fully diluted with water. This might suggest that 1-propanol may not be as efficient as 1-butanol. Moreover, the 1-propanol is very hydrophilic, so it tends to dissolve in the water phase instead of being inserted into the interface layer. Hence, with 1-propanol as a cosurfactant, it occupied a smaller mole fraction among the interfacial layer than 1-butanol, and not enough to allow the solubilization of a high amount of water. In the case of 1-pentanol, the phase diagram undergoes a striking change (Figure 2c). There was no dilution line crossing the entire phase diagram while the area of the single microemulsion region decreased considerably. This may be attributed to the interface film is too rigid to let the droplets merge to form the microemulsion phase. In this

DOI: 10.1021/sc500667n
ACS Sustainable Chem. Eng. 2015, 3, 443−450

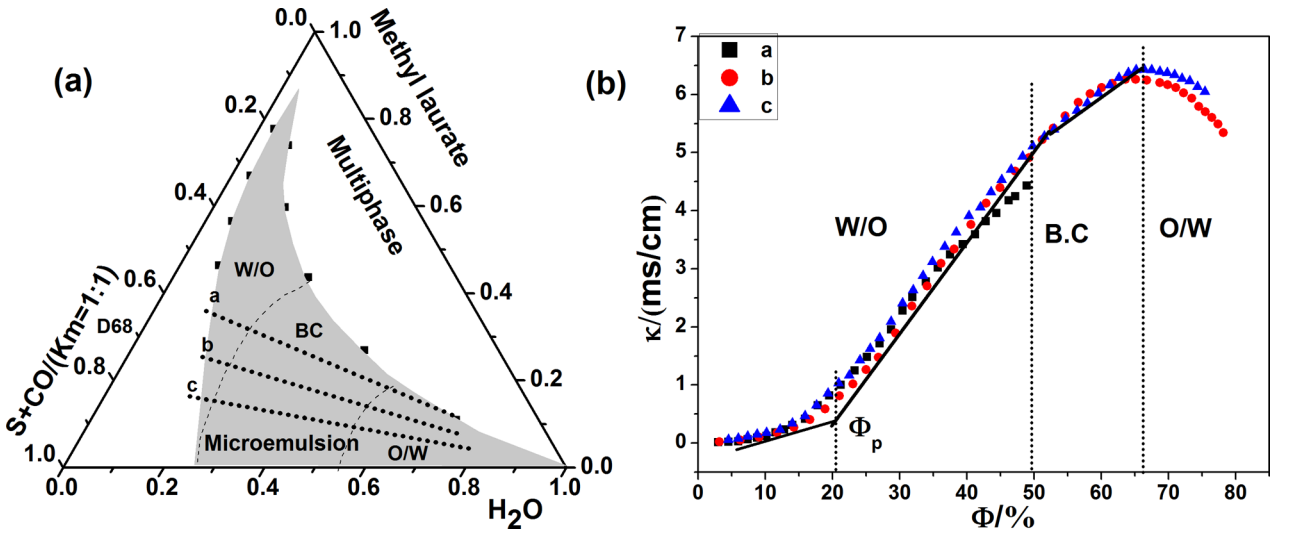

Figure 4. Pusedoternary phase diagram for water/APG-AEC/1-butanol&1-propanal/methyl laurate (APG/AEC = 3/1, 1-butanol/1-propanal = 2/1) is shown in order to associate the topology of the domains of the single phase microemulsion to conductivity. Paths a, b and c describe the three lines upon which conductivity experiments were performed.

section, medium chain alknaol (1-butnaol), as a cosurfactant, is the most efficient at expanding the single phase region.

Effects of the Oil Phase. For a better understanding of the role of the chain length of oil plays in forming the single phase region of microemulsion, palmitic acid methyl ester, methyl laurate, oleic acid methyl ester was selected. The influence of the molecular volume and hydrophobicity of the oil on the phase behavior of the system based on water/APG-AEC/butanol/FAMEs are shown in Figure 3. The APG/AEC weight ratio (3:1) and surfactant/cosurfactant weight ratio (1:1) was kept constant. A phase diagram with two regions was obtained using methyl laurate, namely, liquid crystals (LC) and the single phase region; see Figure 3c. The LC domain was embedded within the microemulsion phase zone the near water-rich corner. This may be interpreted that the interfacial film was too rigid to fluctuate and to allow the transformation between W/O microemulsion and O/W microemulsion. It also proved that a molecule of oil can change interfacial parameters through the partial alkyl chain of oil penetration into hydrophobic chains of the surfactant at the interfacial film. Hence, the LC domain can be removed if 1-butanol is supplemented with propanol due to concomitantly increased fluidity in the interfacial film (Figure 3d). The single phase of microemulsion with oleic acid methyl ester was similar to that with palmitic acid methyl ester, despite the former having a longer alkyl chain (Figure 3a,b). This may be attributed to the dependence of microemulsion formation not only on the geometric parameters but also on chain stiffness. Previous studies have shown that the solubilization capability of hydrocarbon with double bond was significantly higher than that of system with linear hydrocarbons. That can be explain mutual miscibility between the hydrophobic part of the surfactant and alkyl chain of oil will affect the insertion of oil into the amphiphilic film, and will change the spontaneous curvature.[18]

According to the above results, the optimum formulation was composed of APG/AEC (3:1) as the surfactant, 1-butanol/1-propanol (2:1) as the cosurfactant and methyl laurate as the oil phase with R = 7/3.

Property of Optimum Microemulsion. *Conductivity.* Electrical conductivity is a structure-sensitive property, so the structure of microemulsion can be detected through conductivity measurements.[27,28] Figure 4 reveals the electrical conductivity of the optimum microemulsion as a function of the volume faction (Φ_w) of water, which was used as the titration phase for dilution of the microemulsion. It can be found that at lower water contents, the conductance is very small, the value increasing slowly with increasing water fraction. When Φ_w reached a critical point, Φ_p, a so-called percolation threshold, the conductivity started rose sharply to a plateau.[29]

Then, conductivity sharply increased until reaching a plateau with increasing amounts of water. This phenomenon can be explained with percolation model. When water content was below Φ_p, the water-in-oil droplets are embedded in the nonconducting oil phase and isolated from one another, which contributed very little to the electrical conductance.[2] Collision occurs in succession between water-in-oil droplets, during which ions in the core of the droplet can hop from droplet to droplet, so that a small value of conductivity was measured. However, the conductivity of system increases slowly because the number of droplets in the bulk phase is small. On further swelling of the droplet volume with water content, when $\Phi_w > \Phi_p$, contact between droplets occurs and results in the formation of clusters. Due to attractive interactions among the water droplets and the repulsion of ions on the double electric layer, water droplets move closer to one another and form a network of conductive channels. Percolation then occurs and the conductivity suddenly increases. When Φ_w > 53%, the conductivity increases slightly to a maximum $\Phi_w \approx$ 63%). Afterward, the conductivity declines upon further diluting in water. Electrical conductivity results indicate that the structure of the microemulsion transforms from W/O to bicontinuous phase to O/W with the titration of water into the system.[30]

Dilution Stability. The dilution stability of microemulsion is very important for practical applications, such as in pesticide. The optimum formulation with a mass composition of 15% AEC&APG, 15%1-butanol&1-propanal, 20% methyl laurate and 50% water was selected to determine the dilution stability of the microemulsion. After 20-fold and 200-fold dilution with water, the droplet sizes in the dilute solutions were measured using dynamic light scattering (DLS). Figure 5b shows the time

DOI: 10.1021/sc500667n
ACS Sustainable Chem. Eng. 2015, 3, 443−450

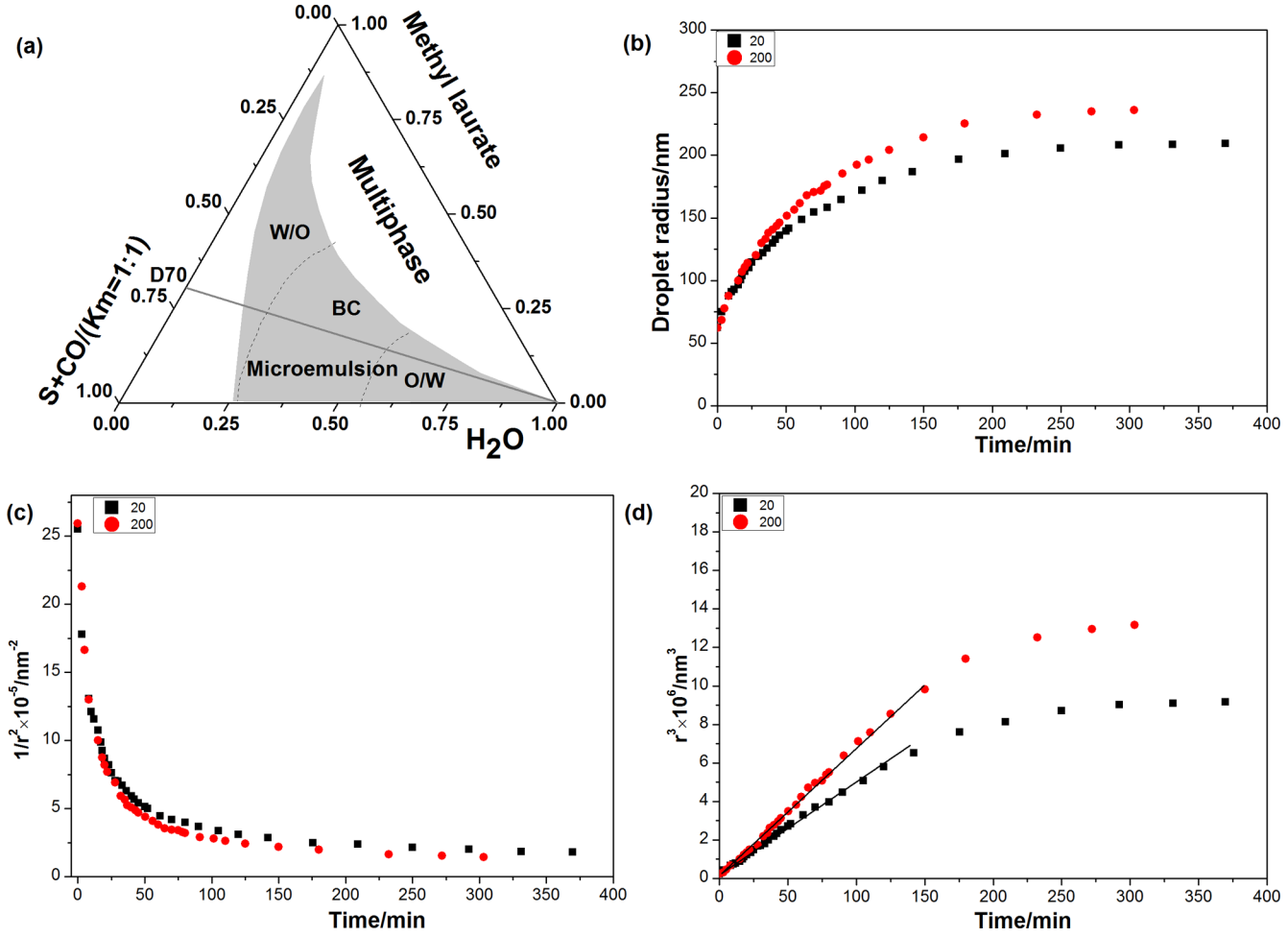

Figure 5. (a) Pseudoternary phase diagram of water/APG-AEC/1-butanol&1-propanol/methyl laurate (APG/AEC = 3/1, 1-butanol/1-propanol = 2/1) is shown in order to associate the topology of the realms of existence of the single phase to dilute solution. The droplet diameter of systems with different dilute times was a function of time (b), and $1/r^2 \sim t$ (c), $r^3 \sim t$ (d).

evolution of the mean particle radius (r). It is clear that increased with time dramatically just after the dilution, and the rate of growth then slows after about 60 min until after 200 min, and the size remained constant. The droplet size after 200-fold dilution is slightly larger than this that after 20-fold dilution. This can be attributed to cosurfactant diffusion from the interface into the aqueous phase upon dilution, leading to rising interfacial tension and increasing free energy with the systems. The droplets of dispersed phase therefore swell to increase the interfacial area and reduce the free energy of the system. However, once the systems reach equilibrium again, the droplet sizes tend to stabilize with time.

To explore the mechanism of instability of the as-prepared microemulsion during the dilution process, the time evolution of $1/r^2$ and r^3 are plotted in Figure 5c,d. Tadros and co-workers[31] predict that if the instability indicates coalescence, $1/r$ should change linearly with time according to the following expression:

$$\frac{1}{r} = r_0^2\left(\frac{8\pi}{3}\right)\omega t \tag{1}$$

where r is the average droplet radius after time t, r_0 is the droplet radius at t_0 and ω is the frequency of rupture per unit surface of the film. It can be seen from Figure 5c that the $1/r^2$ decreases sharply with increasing of time, and therefore coalescence should not be occurring during water dilution.

For Ostwald ripening, previous research has shown that dr^3/dt is given by[32]

$$\omega = \frac{dr^3}{dt} = \frac{8}{9}\frac{C(\infty)\gamma V_m D}{\rho RT} \tag{2}$$

where r is the critical radius, $C(\infty)$ is the bulk phase solubility (the solubility of the oil in an infinitely large droplet), γ is the interfacial tension, V_m is the molar volume of the oil, D is the diffusion coefficient of the oil in the continuous phase, ρ is the oil density and R is the gas constant.[33,34]

Figure 5d indicates that before 150 min, the gradient of r^3 against time is constant, in agreement with eq 2. These results imply that the main driving force for dilute solution instability is Ostwald ripening after the dilution process has begun. During the dilution process, the samples remain monophasic and homogeneous. Therefore, a macroscopically stable dilute solution was obtained.

Spreading Behavior. In applications, such as foliar agrochemical sprays, microemulsions need both to wet and to spread to cover the foliar surface. Spreading is a fundamental observed phenomenon in which the fluid phase is displaced completely or partially on the surface of a solid. The most useful parameter that is typically used to describe spreading is

DOI: 10.1021/sc500667n
ACS Sustainable Chem. Eng. 2015, 3, 443−450

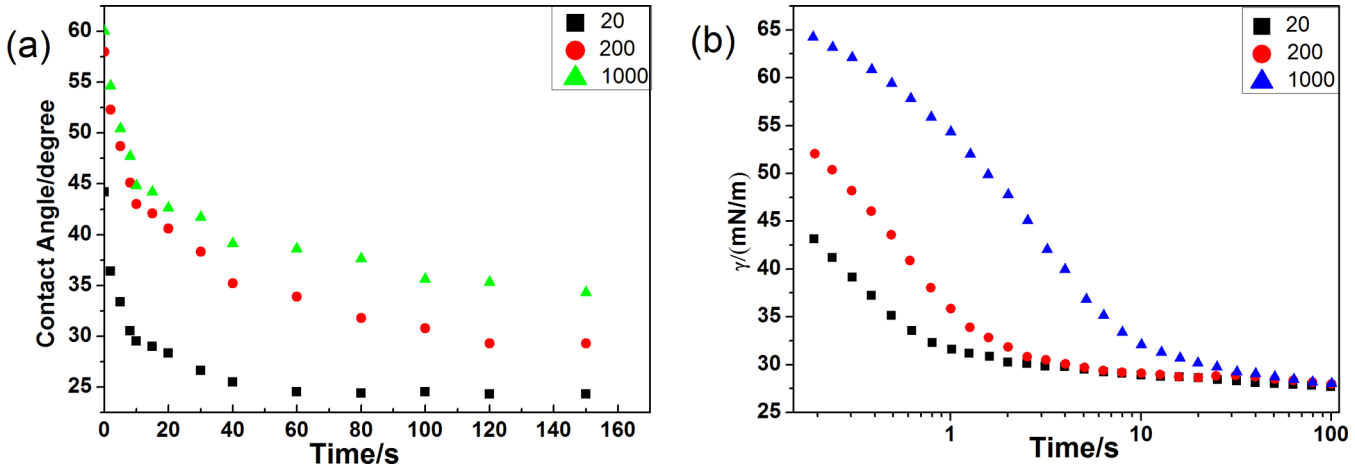

Figure 6. (a) Contact angle for the microemulsions (described in Figure 5a) as a function of time. (b) Dynamic surface tension of the same microemulsion (see Figure 5a) as a function of time.

the contact angle (θ) of a liquid on the substrate. Figure 6 shows the change in contact angle over time against a hydrophobic substrate, paraffin film, for the optimal microemulsion, which was prepared with the same formula as for the measurements of dilution stability and diluted 20-, 200- and 1000-fold in water, respectively. The θ dropped rapidly from 0 to 5 s, after which the rate of decline fell until equilibrium was reached. With the increase of dilution water, the equilibrium value of θ increased. It means that the spreading velocity went up with increasing of the microemulsion concentration. Generally, the spreading behavior on the surface could be divided into two processes: the short time process (fast spreading) and the long time process (slow spreading).[35] The short time process was mainly driven by surface tension gradient along the air/liquid interface.[36] The long time process started from about 5 s to the equilibrium state in which the spreading behavior was controlled by the surfactant diffusion from the bulk to the new surface, and the slopes of the curves decreased with the increase of time and the dilution times.[37] The higher microemusion concentration implied higher surfactant contents leading to faster diffusion from the bulk to the new surface, thus the contact angle reduced more quickly than these for lower microemusion concentration systems.

Dynamic surface tension (γ) is an important surface active property that governs many industrial and biological processes including wetting and spreading.[38] If the dynamic surface tension decays quickly, the drops are more likely to reside on the hydrophobic surfaces. Figure 6b shows the dynamic surface tension (γ) as a function of surface age (t) for the water diluted microemulsion systems we described above. It is clear that increasing the microemulsion concentration results in a faster decay of γ. After 2 s of surface aging, the surface tension of the 200-fold diluted sample had already reached equilibrium, whereas the corresponding 1000-fold diluted sample took 10 s. The gradients of the curves decreased with increasing of surface age, and time, a result consistent with the dynamic contact angle. Both the dynamic surface tension measurements and contact angle results indicate that the optimized microemulsion exhibited excellent spreading performance on hydrophobic substrate even after 1000-fold dilution in water.

CONCLUSION

A fully water dilutable microemulsion with 3:1 (wt %) of APG/AEC as the surfactant, 2:1 (wt %) of 1-butanol/1-propanol as the cosurfactant and methyl laurate as the oil phase was optimized from pseudoternary phase diagrams. It was found that FAMEs could replace toxic and volatile organic solvents as the oil phase, which are widely used in pesticides. The DLS results showed that the droplet size of dilute solutions of the optimized microemulsion increased over time and that the main driving force for this instability was Ostwald ripening. However, the samples remained monophasic and homogeneous throughout the dilution and the droplet size reached a stable plateau after 200 min. It may prove that the macroscopic stable dilute solutions were obtained. The excellent wetting and spreading properties exhibited by diluted microemulsions on hydrophobic surfaces were demonstrated by contact angle and dynamic surface tension measurements. The as-prepared microemulsions have great potential as more environmental friendly microemulsion formulations for industrial and agricultural applications.

AUTHOR INFORMATION

Corresponding Authors

*Zhiping Du. Tel.: +86 3514084691. Fax: +86 3514040802. E-mail: Zhipingdu@sxu.edu.cn.

*Wanxu Wang. Tel.: +86 3514046676. Fax: +86 3514040802. E-mail: ridciwwx@163.com.

Notes

The authors declare no competing financial interest.

ACKNOWLEDGMENTS

This reasearch was funded by the Shanxi Science and Technology Innovation Project (#2012102008), Shanxi Province patent promotion project (#141015), the National Science & Technology Pillar Program during the Twelfth Five-year Plan Period (#2014BAE03B03), National Natural Science Found of China (#21103228) and Natural Science Found of Shanxi Province (#2014011014-1).

REFERENCES

(1) McClements, D. J. Nanoemulsions versus microemulsions: Terminology, differences, and similarities. *Soft Matter* **2012**, *8*, 1719−1729.

DOI: 10.1021/sc500667n
ACS Sustainable Chem. Eng. 2015, 3, 443−450

(2) Klossek, M. L.; Touraud, D.; Kunz, W. Microemulsions with renewable feedstock oils. *Green Chem.* **2012**, *14*, 2017−2023.
(3) Ryan, L. D.; Schubert, K. V.; Kaler, E. W. Phase behavior of microemulsions made with n-alkyl monoglucosides and n-alkyl polyglycol ethers. *Langmuir* **1997**, *13*, 1510−1518.
(4) Fanun, M. *Microemulsions: Properties and Applications*; CRC Press: Boca Raton, FL, 2010.
(5) Engelskirchen, S.; Maurer, R.; Levy, T.; Berghaus, R.; Auweter, H.; Glatter, O. Highly concentrated emulsified microemulsions as solvent-free plant protection formulations. *J. Colloid Interface Sci.* **2012**, *388*, 151−161.
(6) Tamhane, V. A.; Dhaware, D. G.; Khandelwal, N.; Giri, A. P.; Panchagnula, V. Enhanced permeation, leaf retention, and plant protease inhibitor activity with bicontinuous microemulsions. *J. Colloid Interface Sci.* **2012**, *383*, 177−183.
(7) Chin, C. P.; Lan, C. W.; Wu, H. S. Study on the performance of lambda cyhalothrin microemulsion with biodiesel as an alternative solvent. *Ind. Eng. Chem. Res.* **2012**, *51*, 4710−4718.
(8) Zhang, Y.; Zhao, J.; Zhang, S.; Zhong, Y.; Wang, Z.; Liu, Y.; Shi, F.; Feng, N. Enhanced transdermal delivery of evodiamine and rutaecarpine using microemulsion. *Int. J. Manomed.* **2011**, *6*, 2469.
(9) Chudasama, A.; Patel, V.; Nivsarkar, M.; Vasu, K.; Shishoo, C. Investigation of microemulsion system for transdermal delivery of itraconazole. *J. Adv. Pharm. Technol. Res.* **2011**, *2*, 30.
(10) Tsai, Y. H.; Fu, L. T.; Huang, C. T.; Chang, J. S.; Huang, Y. B.; Wu, P. C. Formulation optimization of estradiol microemulsion using response surface methodology. *J. Pharm. Sci.* **2011**, *100*, 4383−4389.
(11) Deutch-Kolevzon, R.; Aserin, A.; Garti, N. Synergistic cosolubilization of omega-3 fatty acid esters and CoQ 10 in dilutable microemulsions. *Chemistry Phys. Lipids* **2011**, *164*, 654−663.
(12) Garti, N.; Yaghmur, A.; Leser, M. E.; Clement, V.; Watzke, H. J. Improved oil solubilization in oil/water food grade microemulsions in the presence of polyols and ethanol. *J. Agric. Food Chem.* **2001**, *49*, 2552−2562.
(13) Zhong, F.; Yu, M.; Luo, C.; Shoemaker, C. F.; Li, Y.; Xia, S.; Ma, J. Formation and characterisation of mint oil/S and CS/water microemulsions. *Food Chem.* **2009**, *115*, 539−544.
(14) Acosta, E. Bioavailability of nanoparticles in nutrient and nutraceutical delivery. *Curr. Opin. Colloid Interface Sci.* **2009**, *14*, 3−15.
(15) Garti, N.; Yaghmur, A.; Aserin, A.; Spernath, A.; Elfakess, R.; Ezrahi, S. Solubilization of active molecules in microemulsions for improved environmental protection. *Colloids Surf., A* **2003**, *230*, 183−190.
(16) Tadros, T. F. *Surfactants in Agrochemicals*; Marcel Dekker: New York, 1995; Vol. *54*.
(17) Kahlweit, M.; Faulhaber, B.; Busse, G. Microemulsions with mixtures of nonionic and ionic amphiphiles. *Langmuir* **1994**, *10*, 2528−2532.
(18) Mehta, S.; Kaur, G.; Mutneja, R.; Bhasin, K. Solubilization, microstructure, and thermodynamics of fully dilutable U-type Brij microemulsion. *J. Colloid Interface Sci.* **2009**, *338*, 542−549.
(19) Solè, I.; Solans, C.; Maestro, A.; González, C.; Gutiérrez, J. Study of nano-emulsion formation by dilution of microemulsions. *J. Colloid Interface Sci.* **2012**, *376*, 133−139.
(20) Von Rybinski, W.; Guckenbiehl, B.; Tesmann, H. Influence of co-surfactants on microemulsions with alkyl polyglycosides. *Colloids Surf., A* **1998**, *142*, 333−342.
(21) Kahlweit, M.; Busse, G.; Faulhaber, B. Preparing micro-emulsions with alkyl monoglucosides and the role of n-alkanols. *Langmuir* **1995**, *11*, 3382−3387.
(22) Sottmann, T.; Kluge, K.; Strey, R.; Reimer, J.; Söderman, O. General patterns of the phase behavior of mixtures of H_2O, alkanes, alkyl glucosides, and cosurfactants. *Langmuir* **2002**, *18*, 3058−3067.
(23) Liangshu, X.; Guowen, P. Study on synthesis and surface activity of sodium laury alcohol polyoxyethylene (9) ether acetate. *Spec. Petrochem. (Tianjin, China)* **2002**, *2*, 002.
(24) Chin, C.; Lan, C.; Wu, H. Application of biodiesel as carrier for insecticide emulsifiable concentrate formulation. *J. Taiwan Instit. Chem. Eng.* **2012**, *43*, 578−584.
(25) Klossek, M. L.; Marcus, J.; Touraud, D.; Kunz, W. The extension of microemulsion regions by combining ethanol with other cosurfactants. *Colloids Surf., A* **2013**, *427*, 95−100.
(26) Klossek, M. L.; Marcus, J.; Touraud, D.; Kunz, W. Highly water dilutable green microemulsions. *Colloids Surf., A* **2014**, *442*, 105−110.
(27) Lagourette, B.; Peyrelasse, J.; Boned, C.; Clausse, M. Percolative conduction in microemulsion type systems. *Nature* **1979**, *281*, 60−62.
(28) Mehta, S.; Bala, K. Tween-based microemulsions: A percolation view. *Fluid Phase Equilib.* **2000**, *172*, 197−209.
(29) Appel, M.; Spehr, T. L.; Wipf, R.; Stühn, B. Water−AOT−alkylbenzene microemulsions: Influence of alkyl chain length on structure and percolation behavior. *J. Colloid Interface Sci.* **2012**, *376*, 140−145.
(30) Clausse, M.; Peyrelasse, J.; Heil, J.; Boned, C.; Lagourette, B. Bicontinuous structure zones in microemulsions. *Nature* **1981**, *293*, 636−638.
(31) Tadros, T.; Izquierdo, P.; Esquena, J.; Solans, C. Formation and stability of nano-emulsions. *Adv. Colloid Interface Sci.* **2004**, *108*, 303−318.
(32) Chebil, A.; Desbrières, J.; Nouvel, C.; Six, J.-L.; Durand, A. Ostwald ripening of nanoemulsions stopped by combined interfacial adsorptions of molecular and macromolecular nonionic stabilizers. *Colloids Surf., A* **2013**, *425*, 24−30.
(33) Spernath, A.; Aserin, A.; Garti, N. Fully dilutable micro-emulsions embedded with phospholipids and stabilized by short-chain organic acids and polyols. *J. Colloid Interface Sci.* **2006**, *299*, 900−909.
(34) Pons, R.; Carrera, I.; Caelles, J.; Rouch, J.; Panizza, P. Formation and properties of miniemulsions formed by microemulsions dilution. *Adv. Colloid Interface Sci.* **2003**, *106*, 129−146.
(35) Tang, X.; Dong, J.; Li, X. A comparison of spreading behaviors of Silwet l-77 on dry and wet lotus leaves. *J. Colloid Interface Sci.* **2008**, *325*, 223−227.
(36) Nikolov, A. D.; Wasan, D. T.; Chengara, A.; Koczo, K.; Policello, G. A.; Kolossvary, I. Superspreading driven by Marangoni flow. *Adv. Colloid Interface Sci.* **2002**, *96*, 325−338.
(37) Von Bahr, M.; Tiberg, F.; Zhmud, B. V. Spreading dynamics of surfactant solutions. *Langmuir* **1999**, *15*, 7069−7075.
(38) Eastoe, J.; Dalton, J. Dynamic surface tension and adsorption mechanisms of surfactants at the air−water interface. *Adv. Colloid Interface Sci.* **2000**, *85*, 103−144.

DOI: 10.1021/sc500667n
ACS Sustainable Chem. Eng. 2015, 3, 443−450